Springer

Journal of Mechanical Science and Technology 23 (2009) 3161~3168

Journal of Mechanical Science and Technology

www.springerlink.com/content/1738-494x
DOI 10.1007/s12206-009-0917-z

Bending properties for composites with wrinkled and overlapped fabric preform †

Thanh Trung Do and Dong Joo Lee*

School of Mechanical Engineering, Yeungnam University
214-1, Daedong, Gyeongsan-si, Gyeongsangbuk-do, 712-714, Korea

(Manuscript Received November 18, 2008; Revised August 13, 2009; Accepted August 13, 2009)

Abstract

The fiber fabric layers in a preform can be wrinkled or overlapped during a preform loading of the resin transfer molding and thermoforming processes of thermoplastic composites. These fabric discontinuities affect both the mechanical properties and failure mechanisms of those composites. Based on the energy method, the analytical bending modulus is considered and compared to the experimental data for several wrinkling and overlapping patterns. Also, those effects on the bending properties are described through the effective parameters, α, which are the wrinkled parameter and overlapped parameter. It is found that the large fiber content and stress concentrations near discontinuity are the reasons for the larger bending moduli of the wrinkled and overlapped models. As a function of the wrinkled length to the span length (L_W/L) and the overlapped length to the span length (L_O/L), respectively, the bending strengths and failure mechanisms show the two stages. This is due to not only the failure modes but also the geometrical structures of the fiber fabric preform.

***Keywords*:** Composites; Resin transfer molding; Wrinkling; Overlapping; Bending modulus and strength

1. Introduction

Resin Transfer Molded Composites (RTMCs) are manufactured through four steps: fiber fabric preform loading, resin injection, curing and demolding. The dry fiber fabric is first preformed into a closed mold, and then the polymer matrix is injected in the form of liquid resin through the inlet into the cavity while the air escapes from the mold through the vent. After curing, the finished part is demolded [1-6]. During the preform loading process, wrinkled or overlapped fiber fabric layers easily occur and can be a source of crack initiation in the RTMCs. However, the effects of wrinkling and overlapping on the mechanical properties have not yet been studied.

Also, the laminar composites have some inevitable problems due to the wrinkled and overlapped patterns for different geometric shapes, stacking sequences and material stiffness. Even though the advantages of laminar fabric composites are not fully understood in terms of their elastic properties, the uses of these composites has increased recently due to many advantages such as low manufacturing cost, high fracture toughness and the processing technique, etc. However, due to the wrinkling and overlapping, the mechanical properties of these composites can also be significantly degraded.

Several authors have worked on the manufacturing and performance of RTMCs by describing the structure of the fiber fabric preform, including Holmberg and Berglund [7] who studied the problems of the preform for both U-beam and tensile failure mechanisms and concluded that the fabric fibers of the preform can be discontinued during preforming and/or mold closure. This caused the problem of void content for the finished composite.

† This paper was recommended for publication in revised form by Associate Editor Chongdu Cho

*Corresponding author. Tel.: +82 53 810 2469, Fax.: +82 53 813 3703
E-mail address: djlee@yu.ac.kr

The objective of this paper is to determine the bending properties of composites with different wrinkled and overlapped preform patterns using a three-point bend test and then comparing these results to the normal preform. Based on the energy method, the bending modulus is analyzed and compared with the experimental data in order to determine the effects of both wrinkled and overlapping preform types. In addition, the failure mechanisms due to the geometrical structures and failure modes are considered in this study.

2. Analytical model

A specimen used in the test is modeled as a simply supported beam of a constant thickness t, width b and span length L. The structure of the specimen has a few wrinkled layers with a wrinkled length L_W or a few overlapped layers with an overlapped length L_O, which can generally be described by an effective length L_e. The bending moduli of the wrinkling and overlapping sections are E_2 for the normal factor and G_2 for the shear factor. The non-wrinkling and non-overlapping sections have bending moduli of E_1 and G_1 for the normal and shear factors, respectively. For a constant rectangular cross-section, the moment of inertia of the specimen is

$$I = \frac{bt^3}{12} \tag{1}$$

A three-point bending is considered, and the specimen is subjected to a load P applied at its mid-span, as is shown in Fig. 1.
Based on the energy method,

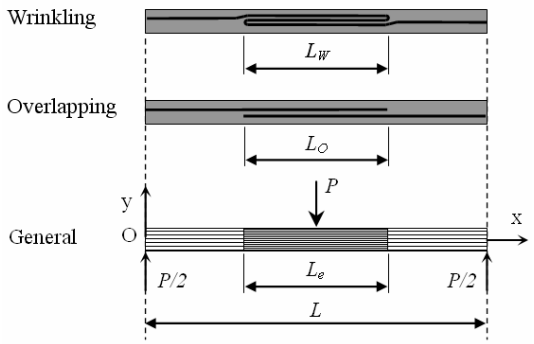

Fig. 1. Model used in the analytical study.

$$U_{normal} = 2\left(\int_0^{\frac{L-L_e}{2}} \frac{M_x^2}{2E_1 I}dx + \int_{\frac{L-L_e}{2}}^{\frac{L}{2}} \frac{M_x^2}{2E_2 I}dx\right)$$
$$= \frac{P^2}{8bt^3}\left(\frac{(L-L_e)^3}{E_1} + \frac{L^3-(L-L_e)^3}{E_2}\right) \tag{2}$$

$$U_{shear} = 4\left(\int_0^{\frac{L-L_e}{2}}\int_0^{\frac{t}{2}} \frac{\tau^2}{2G_1}bdydx + \int_{\frac{L-L_e}{2}}^{\frac{L}{2}}\int_0^{\frac{t}{2}} \frac{\tau^2}{2G_2}bdydx\right)$$
$$= \frac{3P^2}{20bt}\left(\frac{L-L_e}{G_1} + \frac{L_e}{G_2}\right) \tag{3}$$

In a three-point bending mode, both the normal stress and shear stress components are presented throughout the beam span [8]. Therefore, if contributions from both stresses are taken into account, the total energy is

$$U = U_{normal} + U_{shear}$$
$$= \frac{P^2}{8bt^3}\left(\frac{(L-L_e)^3}{E_1} + \frac{L^3-(L-L_e)^3}{E_2} + \frac{6}{5}t^2\left(\frac{L-L_e}{G_1} + \frac{L_e}{G_2}\right)\right) \tag{4}$$

The total deflection at the mid-span of the beam is

$$\delta = \frac{2U}{P}$$
$$= \frac{P}{4bt^3}\left(\frac{(L-L_e)^3}{E_1} + \frac{L^3-(L-L_e)^3}{E_2} + \frac{6}{5}t^2\left(\frac{L-L_e}{G_1} + \frac{L_e}{G_2}\right)\right) \tag{5}$$

The bending moduli of the specimen as a function of both wrinkled length and overlapped length are

$$\frac{(L-L_e)^3}{E_1} + \frac{L^3-(L-L_e)^3}{E_2} + \frac{6}{5}t^2\left(\frac{L-L_e}{G_1} + \frac{L_e}{G_2}\right) = \frac{4\delta bt^3}{P} \tag{6}$$

where $G = \frac{E}{2(1+\nu)}$ and ν is Poisson's ratio.

Strictly speaking, this equation can be used for either an isotropic material or used with a caution for a material having "fiber" symmetry as in woven or cross-plied at 0^0 and 90^0 fiber reinforcement.

The shear pattern can be reduced by employing a high span-thickness (L/t) ratio for the beam laminate composite and Eq. (6) can be rewritten as

$$\frac{(L-L_e)^3}{E_1} + \frac{L^3-(L-L_e)^3}{E_2} = \frac{4\delta bt^3}{P} \tag{7}$$

If the structure of the specimen has both non-wrinkling and non-overlapping layers, i.e., $L_e = 0$ and $E_1 = E_2 = E$, and the shearing as a high span-thickness ratio is ignored, the above equations can be expressed as given in Eq. (8). This equation can also be applied for the general beam without the consideration of its geometrical structure.

$$\delta = \frac{2U}{P} = \frac{PL^3}{4Ebt^3} \quad \text{and} \quad E = \frac{PL^3}{4\delta bt^3} \tag{8}$$

3. Experimental

The materials prepared for these experiments are Polyester resin R235 (density $\rho = 1.05$ g/cm^3, bending modulus $E = 3$ GPa and bending strength with shear factor $\sigma_{max} = 59$ MPa) from Sewon chemical Co. and E-glass woven fabric K618 ($\rho = 2.54$ g/cm^3, $E = 70$ GPa and $\sigma_{max} = 3.4$ GPa) from Hankuk Fibers Co. The hardener material Luperox DDM from Seki Arkema Co. is mixed with the resin in a ratio of 1:120 (g) to reduce the curing time.

The specimen used in this study is modeled as a simply supported beam of a rectangular cross-section with thickness $t = 2.1$ mm and width $b = 33.3$ mm. In addition, the geometrical structures of the fabric preform types have several models, which are normal, wrinkling and overlapping, as is shown in Fig. 2.

- Model 1 is a normal type. The fiber fabric preform has different numbers of continuous layers: 2, 4, 6 and 8 layers.
- Models W-1, W-2 and W-3 are wrinkled preform types with different numbers of wrinkled layers; 1, 2 and 3, respectively.
- Models O-1, O-2 and O-3 are overlapped preform models with different numbers of overlapped layers; 1, 2 and 4, respectively.

Typically, the ratios of the wrinkled length to the span length (L_W/L) and the overlapped length to the span length (L_O/L) are considered from 0.05 to 0.9. The test specimens are cut by an electric band saw from the original plate sample of 300 mm x 200 mm. Three-point bend tests are performed with a constant span length of $L = 100$ mm, as is shown in Fig. 3. All tests were done using a Shimazu machine at a testing speed of 5 mm/min. at room temperature and at a relative humidity of 50%. Three specimens are used for a single evaluation.

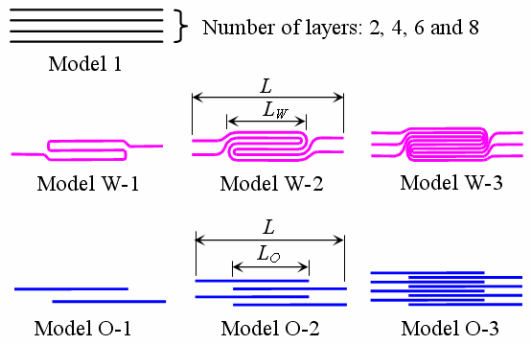

Fig. 2. Fiber preform models.

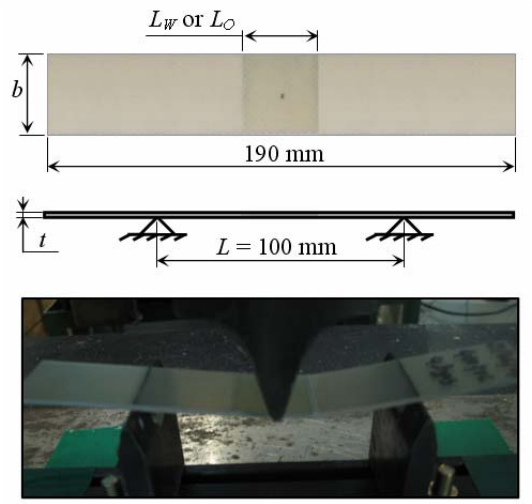

Fig. 3. Specimen and set-up of a three-point bend test.

4. Results and discussion

4.1 Bending modulus

The shear factor can be ignored for analyzing the elastic bending modulus due to a larger span-thickness (L/t) ratio of 47.6:1 and the effects of the energy considering the shear factor on the general energy was below 3% from the experimental results on the elastic period. Therefore, the bending modulus can be determined based on the normal stress using Eq. (8).

Fig. 4 shows the experimental bending moduli of the wrinkled and overlapped models as a function of the wrinkled and overlapped lengths. As expected, the results increased almost linearly with an increasing L_W/L and L_O/L, and exhibit a stiff slope for the preform types with a larger number of wrinkled and overlapped layers or a higher fiber volume fraction (V_f). Fig. 5 compares the bending moduli for different

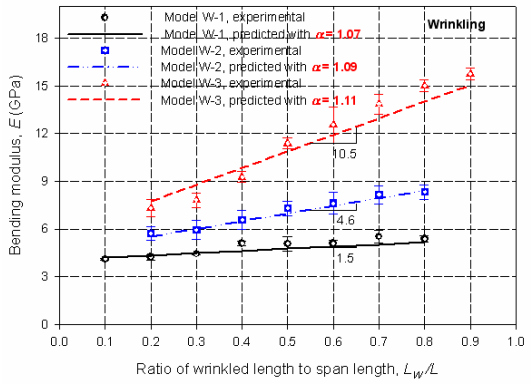

(a) Bending modulus versus L_W/L

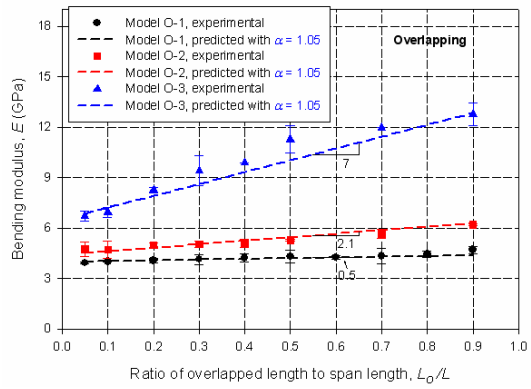

(b) Bending modulus versus L_O/L

Fig. 4. Analytical and experimental bending moduli; (a) for wrinkling, (b) for overlapping.

preform types versus V_f, which was determined using the density of the matrix, fiber and composite. In this comparison, half of the measured V_f is used since the effective fibers are only 50% of the fibers in the fabric preform. It is observed that the bending moduli of the wrinkled and overlapped models are larger than those of the normal model, which is due to the fiber concentration at the mid-span of the beam and an increase in V_f. It is clear that the wrinkled or overlapped preform patterns can be expected in some cases with a higher bending modulus.

In order to consider the effects of the wrinkled and overlapped lengths on the bending modulus, Eq. (7) is considered for the relationship between E_1 and E_2. When $L_e/L = 0$, $E_1 = E$ and when $L_e/L = 1$, $E_2 = E$. In those cases, Eq. (7) can be rewritten as Eq. (8) with those boundary conditions being applied. For $0 < L_e/L < 1$, the experimental bending modulus increased linearly with an increasing wrinkled length or overlapped length. Therefore, the bending modulus can be predicted with the following equation:

$$E = \alpha\left(E_1^*\left(1-\frac{L_e}{L}\right)+E_2^*\frac{L_e}{L}\right) \tag{9}$$

where α is an effective parameter due to wrinkling and overlapping, E^*_1 is the predicted modulus corresponding the non-wrinkling or non-overlapping sections and E^*_2 is the predicted modulus corresponding the wrinkling or overlapping sections.

E^*_1 and E^*_2 are the constant values that can be predicted from the normal preform type (Model 1) with a given number of layers, as is shown in Fig. 5. For the wrinkled preform types, the predicted values of E^*_1 are 3.8 GPa, 4.2 GPa and 5.1 GPa, and those of E^*_2 are 5.1 GPa, 8.6 GPa and 14.5 GPa; for Models W-1, W-2 and W-3, respectively. Similarly, the values of E^*_1 are 3.8 GPa, 4.2 GPa and 6.2 GPa, and those of E^*_2 are 4.2 GPa, 6.2 GPa and 12.5 GPa; for Models O-1, O-2 and O-3, respectively, for the overlapped preform types.

Due to the fiber concentration in the wrinkling and overlapping sections where a load P is applied at the mid-span of the specimen, the fiber volume fractions of the wrinkled and overlapped models are larger than those of the normal model as a function of the number of layers. The moduli of those sections are also larger than those of the non-wrinkling and non-overlapping sections, so it can be assumed that $E_1 = \alpha E^*_1$ and $E_2 = \alpha E^*_2$. The effective parameter (α) is reasonable with a positive number. Based on the analytical results, as described in Figs. 3 and 4, the wrinkled parameters α are 1.07, 1.09 and 1.11 for Models W-1, W-2 and W-3, respectively, and the overlapped parameter is 1.05 for all overlapped models. These values are due to both the fiber concentration and the geometrical structures of the wrinkled/overlapped fabric preform. The structure of the wrinkled preform models was all the wrinkled layers by combination. However, the structure of the overlapped models was a one-by-one overlapped layer. In addition, the fiber volume fractions of the wrinkled models are larger than those of the overlapped models as a function of the number of layers. Therefore, the trend of the wrinkled parameter tends to increase with an increasing number of wrinkled layers. However, this was a constant value for the overlapped models with a given number of overlapped layers. As is shown in Fig. 4, it can be seen that the predicted results using Eq. (9) are in good

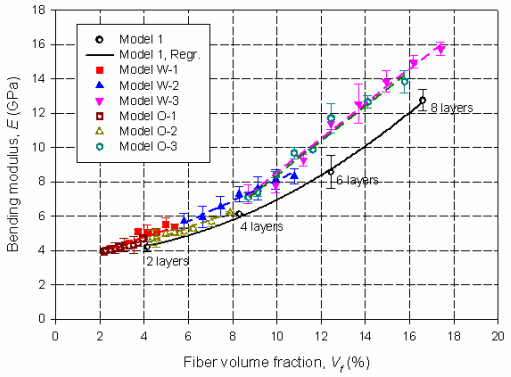

Fig. 5. Comparison of the bending moduli for normal, wrinkled and overlapped models.

agreement with the analytical results using Eq. (7) and are also satisfied with the experimentally measured data. As expected, the bending modulus and the effective parameter for the other models with various numbers of layers and effective length can be determined.

4.2 Bending strength

Assuming the specimen is a homogenous beam, the bending strength with the shear factor in a three-point bend test is given by [8]

$$\sigma_{\max} = \frac{3P_{\max}L}{2bt^2}\left(1+6\left(\frac{\delta}{L}\right)^2-4\left(\frac{t}{L}\right)\left(\frac{\delta}{L}\right)\right) \tag{10}$$

Figs. 6a and 6b show the measured bending strengths for the maximum stresses considering the shear factor for the whole laminate composite specimens as a function of the wrinkled and overlapped lengths, respectively. The bending strengths have two stages with an increasing L_W/L and L_O/L, and they are shown as the peeling layers for stage (I) and as the breaking fibers or the achieved maximum fiber stress for stage (II). For the first stage (I), the bending load increased almost linearly with deflection up to the final failure. The maximum stress was the same as the failure stress when the bending load was at its maximum value. In this stage, Mode I (opening mode) is the main cause of the specimen failure due to the failure of the interfacial bond for the wrinkling and overlapping sections, which occurred before the fibers achieve their potential strength, as is shown in Figs. 8a and 8b. This can be described as the following equation:

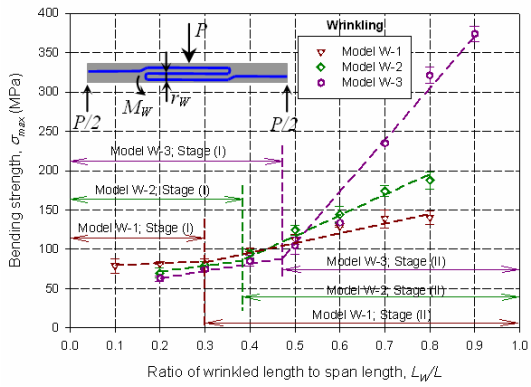

(a) Bending strength versus L_W/L

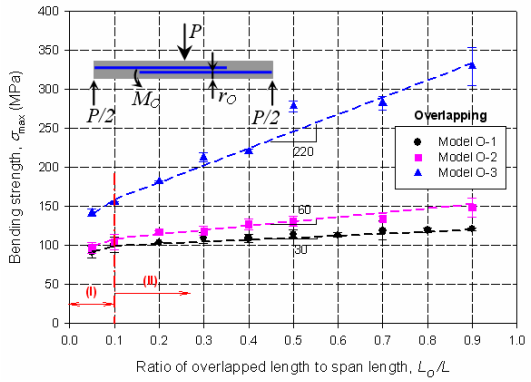

(b) Bending strength versus L_O/L

Fig. 6. Analytical and experimental bending strengths; (a) for wrinkling, (b) for overlapping.

$$\sigma_{\max} = \frac{M_e}{I}r_e = \frac{12r_eP_{\max}}{bt^3}\left(1-\frac{L_e}{2L}\right)\left(\frac{L_e}{2}\right) \tag{11}$$

where M_e is the moment of the wrinkled or overlapped bond area, and r_e are values of (2/3)t and (1/2)t for the wrinkling and overlapping sections, respectively.

For the second stage (II), the wrinkled and overlapped lengths reached values that were deemed large values and the interfacial bond became strong enough without peeling failure under the three-point bend test. The specimen obtained the bending strength as the maximum stress when it was either the breaking fiber in Figs. 7b and 7e, or the achieved maximum fiber stress at the outermost layers, which is shown in Figs. 7c and 7f. In those cases, the bending strength is calculated by Eq. (10).

In general, both the fiber stress and interfacial bond stress of the wrinkling and overlapping sections are

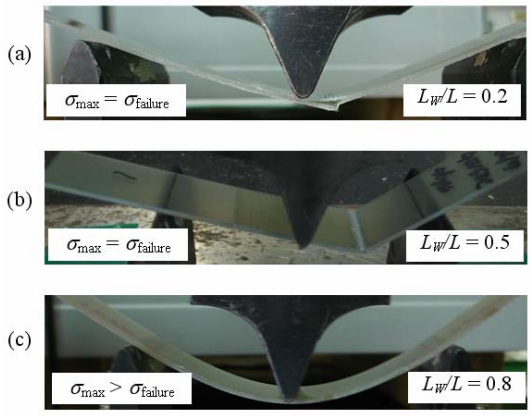

Model W-3

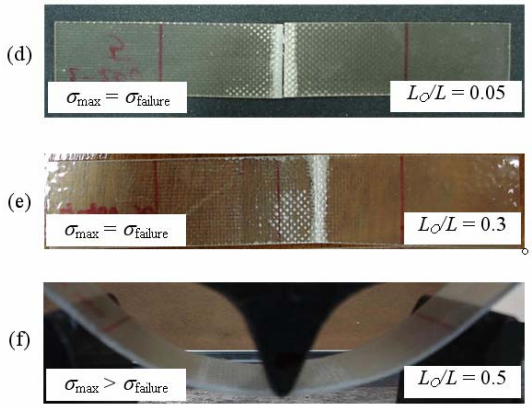

Model O-3

Fig. 7. Effects of the wrinkled and overlapped lengths on the failure mechanisms.

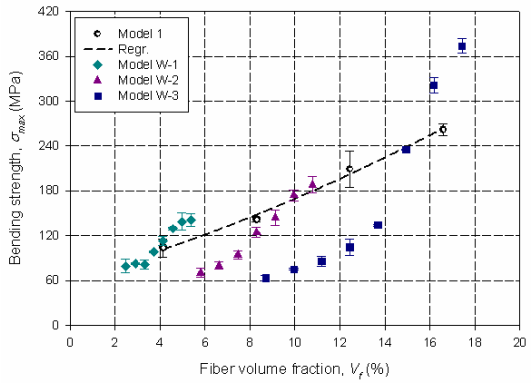

(a) Wrinkled and normal models

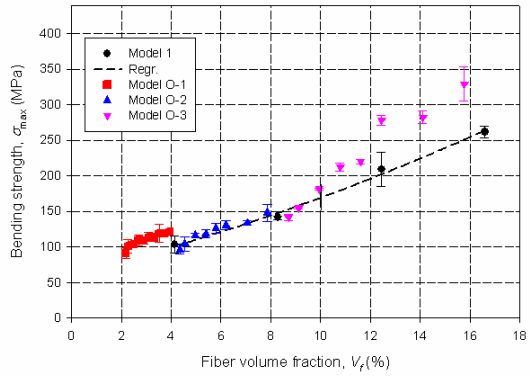

(b) Overlapped and normal models

Fig. 8. Bending strengths versus V_f for normal, wrinkled and overlapped models.

present throughout the beam span in the three-point bend test. If the contributions from both stresses are taken into account, the bending strength as the total maximum stress of the beam specimen is

$$\sigma_{\max}\Big|_{L_e} = \frac{P_{\max}}{bt^2}\left(\frac{12r_e}{t}\left(1-\frac{L_e}{2L}\right)\left(\frac{L_e}{2}\right) + \frac{3L}{2}\left(1+6\left(\frac{\delta}{L}\right)^2 - 4\left(\frac{t}{L}\right)\left(\frac{\delta}{L}\right)\right)\right) \quad (12)$$

where P_{max}, r_e and δ are the values that depend on the wrinkling and overlapping patterns, as are shown in Eq. (7). Typically, the bending strength not only depends on the stiffness of the materials but also on the geometrical structures of the specimen under a three-point bend test. When the structure of the laminate composite was both non-wrinkling and non-overlapping layers, i.e., $L_e = 0$ and $r = 0$ or $L_e = L$, then Eq. (12) is corrected with Eq. (10). It is clear that the boundary conditions are appropriate in this case.

Figs. 8a and 8b compare the bending strengths between the normal and wrinkled models, and the normal and overlapped models versus V_f, respectively. Due to the failure modes, the bending strengths of the wrinkled and overlapped models for stage (I) were almost smaller than those of the normal model. It is clear that the interfacial bond stresses of the wrinkling and overlapping sections achieved the maximum stress before the fibers of the beam achieved their potential stress. Due to the geometrical structure types of the wrinkled and overlapped models, the beam specimens are broken at the ends of the wrinkling and overlapping sections when their lengths were small, as are shown in Figs. 7b, 7e and 8.

In those cases, the ends of wrinkling and overlapping sections achieved their maximum stress. When the wrinkled and overlapped lengths reached the

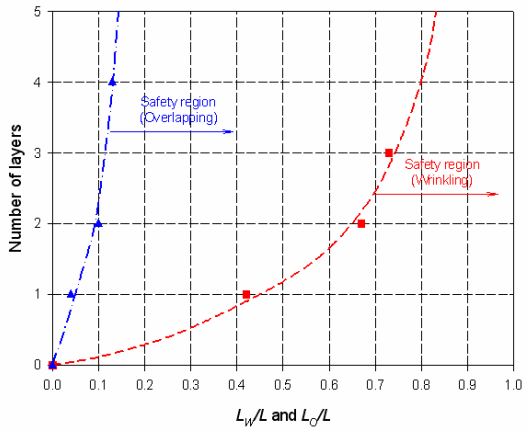

Fig. 9. Safety values of L_W/L and L_O/L versus number of layers.

values that are large enough as $\sigma_{max} > \sigma_{failure}$, the bending strengths of the wrinkled and overlapped models were larger than that of the normal model. This is due to the fibers concentration of the fiber preform models with the wrinkling and overlapping effects. As expected, the safe predicted bending strengths are determined based on those results and are shown in Fig. 9. For a larger number of wrinkled and overlapped layers, the failure strengths due to the stiff materials and the geometrical structure types were larger. For the safety region, the bending strengths of the wrinkled and overlapped models were larger than those of the normal model due to the effects of fiber concentration at the middle of the specimens.

5. Conclusions

The main conclusions drawn from this study are:

(1) A simple method of analysis is developed to analyze the bending properties of composites having both wrinkling and overlapping effects.

(2) The bending modulus increases with an increasing V_f for the laminate composites even though the preform has both wrinkled and overlapped layers. Due to the fiber concentration, the results of the wrinkled and overlapped models are larger than those of the normal model.

(3) The effects of the wrinkling and overlapping on the bending modulus are described by the wrinkled and overlapped parameters, respectively. The trend of the wrinkled parameter tends to increase with an increasing number of wrinkled layers. However, this is a constant value for the overlapped models. These characteristics were due to both the fiber concentration and the geometrical structure of the fabric preform.

(4) The bending strengths of the wrinkled and overlapped fabric preform patterns have two mechanism stages as a function of L_W/L and L_O/L, respectively. As expected, the safe predicted bending strengths for the wrinkling and overlapping models are determined in this study.

Acknowledgment

This research was supported by the research grants of Yeungnam University in 2007.

References

[1] K. F. Karlsson and B. T. Astrom, Manufacturing and applications of structural sandwich components, *Composites Part A* 28 (1997) 97-111.

[2] B. Yang, V. Kozey, S. Adanur and S. Kumar, Bending, compression, and shear behavior of woven glass fiber-epoxy composites, *Composites: Part B* 31 (2000) 715-721.

[3] R. J. Day, P. A. Lovell and A. A. Wazzan, Toughened carbon/epoxy composites made by using core/shell particles, *Composites Science and Technology* 61 (2001) 41-56.

[4] J. M. Lawrence, P. Fried and S. G. Advani, Automated manufacturing environment to address bulk permeability variations and race tracking in resin transfer molding by redirecting flow with auxiliary gates, *Composites Part A* 36 (2005) 1128-1141.

[5] M. Deleglise, Christophe Binetruy and Patricia Krawczak, Solution to filling time prediction issues for constant pressure driven injection in RTM, *Composites Part A* 36 (2005) 339-344.

[6] A. Cheung, Y. Yu and K. Pochiraju, Three-dimensional finite element simulation of curing of polymer composites, *Finite Elements in Analysis and Design* 40 (2004) 895-912.

[7] J. A. Holmberg and L. A. Berglund, Manufacturing and performance of RTM U-beams, *Composites Part A* 28 (1997) 513-521.

[8] P. K. Mallick, *Fiber-reinforced Composites*, Marcel dekker, New York, USA, (1988).

Thanh Trung Do received his B.S. degree in Mechanical Engineering from University of Technical Education HoChiMinh City in Vietnam on March 2000. He then received his M.S. degree on September 2003 and Ph.D. degree on August 2009 from Yeungnam University, Korea, where he is currently post-doctoral fellow. He is also member of University of Technical Education HoChiMinh City, Vietnam.
Email: thanhtrungspkt@yahoo.com

Dong Joo Lee received his B.E. degree in Mechanical Engineering from Yeungnam University, Korea, in 1979. He then received his M.S. and Ph.D. degrees from University of Massachusetts at Amherst in 1983 and 1987, respectively. Between 1987 and 1992, he was a research scientist at Honeywell Inc. in N.J. He is currently a Professor at the School of Mechanical Engineering at Yeungnam University. His research interests focus on polymer matrix composites, experimental mechanics and smart materials.